



Universiteit
Leiden
The Netherlands

Discovery of novel inhibitors to investigate diacylglycerol lipases and α/β hydrolase domain 16A

Janssen, F.J.

Citation

Janssen, F. J. (2016, December 1). *Discovery of novel inhibitors to investigate diacylglycerol lipases and α/β hydrolase domain 16A*. Retrieved from <https://hdl.handle.net/1887/44705>

Version: Not Applicable (or Unknown)

License: [Licence agreement concerning inclusion of doctoral thesis in the Institutional Repository of the University of Leiden](#)

Downloaded from: <https://hdl.handle.net/1887/44705>

Note: To cite this publication please use the final published version (if applicable).

Cover Page



Universiteit Leiden



The handle <http://hdl.handle.net/1887/44705> holds various files of this Leiden University dissertation

Author: Janssen, Freek J.

Title: Discovery of novel inhibitors to investigate diacylglycerol lipases and α/β hydrolase domain 16A

Issue Date: 2016-12-01

Discovery of 1,2,4-triazole sulfonamide ureas as *in vivo* active α/β hydrolase domain type 16A inhibitors*

Introduction

Phospholipids constitute a class of small-molecules, which are located in and impart structural integrity to membranes of mammalian cells. They may also serve as important signaling molecules. Phosphatidylcholine (PC) and phosphatidylethanolamine (PE) are the most abundant phospholipids, whereas phosphatidylserine (PS), phosphatidic acid (PA) and phosphatidylinositol (PI) constitute quantitatively minor classes.¹ PS is located primarily in the inner leaflet of the cell membrane and its externalization (loss of symmetry) is considered a common signal for apoptosis and macrophage phagocytosis.² Moreover PS is known to activate intracellular enzymes, including protein kinase C³ and is involved in blood coagulation.⁴

PS is ubiquitously present in all mammalian cell types, although it is most abundant in brain tissue.¹ Here, PS formation occurs by *L*-serine base exchange from membrane PC and PE by PS synthase-1 and 2 (PSS1 and PSS2), respectively, within the endoplasmic reticulum.¹ Several phospholipases are involved in the degradation of PS. Different phospholipases can either hydrolyse fatty acid esters at the *sn*-1 or *sn*-2 position, cleave the glycerol-phosphate or serine-phosphate bond. In addition, PS can be converted to PE by the mitochondrial enzyme PS decarboxylase. The exact contribution of each of these enzymes to the physiological role of PS remains poorly understood. Recently, a novel enzyme has been

* This research has received support from the Innovative Medicines Initiative Joint Undertaking under grant agreement n° 115489, resources of which are composed of financial contribution from the European Union's Seventh Framework Programme (FP7 / 2007-2013) and EFPIA companies in-kind contribution. Alex van der Ham is kindly acknowledged for all inhibitor optimization and characterization and for help with the biological evaluation of the compounds reported in this chapter. Hui Deng, Juan Zhou and Bobby Florea are kindly acknowledged for their help with the *in vivo* studies in mice.

identified in regulating PS levels; the serine hydrolase α/β hydrolase domain type 16A (ABHD16A also known as BAT5).⁵ The development of ABHD16A knockout mice in combination with a small molecule ABHD16A inhibitor, have characterized ABHD16A as a principal PS lipase. ABHD16A cleaves the fatty acyl chain specifically at the *sn*-1 position (Figure 1A), forming *lyso*-PS as a main product.⁵ *Lyso*-PS is an important signaling phospholipid involved in T-cell growth,⁶ mast cell activation^{7,8} and neurite outgrowth.⁹ Although ABHD16A is ubiquitously expressed throughout the body, it has a relatively high expression in the brain, consistent with the levels of its PS substrate.¹⁰ Within the brain, mRNA studies show high expression of ABHD16A in the cerebellum, a region mostly involved in fine motor movement and in some cognitive skills.¹¹ In addition, site specific mutations in the ABHD16A gene are associated with Kawasaki's disease,¹² an autoimmune disease characterized by inflammation of the blood vessels, known as vasculitis. Interestingly, *in vitro* studies have shown that ABHD16A exhibits monoacylglycerol lipase activity.¹³ Savinainen *et al.* showed that catalytically active ABHD16A overexpressed in HEK293T cells hydrolysed several medium and long chain monoacylglycerols, as assessed by a multi-enzyme cascade fluorescent glycerol assay.¹³ The exact role of this dual ABHD16A function *in vivo* is not known to date.

Lyso-PS is a toll like receptor 2 (TLR2) agonist,¹⁴ and is involved in immune responses. α/β Hydrolase domain type 12 (ABHD12) hydrolyses *lyso*-PS, as reported by Blankman *et al.*¹⁵ ABHD12^{-/-} mice accumulated several distinct long chain *lyso*-PS lipids in the brain. Human genetic studies identified null-mutations of ABHD12 as the cause for the onset of a rare neurological disease that causes polyneuropathy, hearing loss, ataxia, retinitis pigmentosa and cataract (PHARC).^{16,17} ABHD12 knockout studies confirmed that mice devoid of ABHD12 activity suffered from neuroinflammation and displayed multiple symptoms of PHARC.¹⁵ ABHD12^{-/-} mice may, therefore, serve as an excellent mouse model to investigate this neurological disease.¹⁵ The exact molecular mechanism of the development of PHARC is currently unknown, but the accumulation of *lyso*-PS and subsequent excessive signaling via TLR2 are hypothesized to be involved in the neuroinflammatory response. To test this hypothesis, selective and *in vivo* potent inhibitors for ABHD16A, which are predicted to reduce the formation of *lyso*-PS, are required. If this hypothesis can be validated, then substrate reduction therapy by lowering *lyso*-PS levels through ABHD16A inhibition may serve as a potential treatment for PHARC patients.

Currently, three different chemotypes of ABHD16A inhibitors have been reported. Profiling of serine hydrolase inhibitors by Hoover *et al.* identified methylarachidonoyl-fluorophosphonate (**1**, MAFP, Figure 1B) and β -lactone tetrahydrolipstatin (**2**, THL, Figure 1B) as potent ABHD16A inhibitors.¹⁸ The β -lactone activity-based probe (ABP) MB064, efficiently labelled ABHD16A in mouse brain proteomes.¹⁹ Using this ABP, 1,3,4-oxadiazolone LEI103 (**3**, Figure 1B) was discovered as a non-selective ABHD16A inhibitor by Baggelaar *et al.*, 2013. Savinainen *et al.* further explored 1,3,4-oxadiazolones as ABHD16A inhibitors and their hit optimization efforts resulted in the discovery of C7600 (**4**, Figure 1B).¹³ Neutral cholesterol

ester hydrolase 1 (KIAA1363) was observed as an important off-target of C7600 (**4**). Camara *et al.* reported on the development of α -methylene- β -lactone derivatives as serine hydrolase inhibitors.²⁰ Activity-based protein profiling (ABPP) using broad-spectrum probe carboxytetramethylrhodamine fluorophosphonate (TAMRA-FP) led to the discovery of KC01 (**5**), a highly potent ABHD16A inhibitor and its corresponding paired control compound KC02 (**6**, Z/E: 4:1, Figure 1B), that did not inhibit ABHD16A.^{5,20} All three ABHD16A inhibitor chemotypes presumably act as irreversible inhibitors, reacting with the catalytic Ser355, using their warhead (*i.e.* electrophilic trap) as site of covalent attachment. These three chemotypes are not selective and lack bioavailability, thus there is a need for selective and *in vivo* active ABHD16A inhibitors.

A high throughput screening campaign was initiated to discover *sn*-1 diacylglycerol lipase α (DAGL α) inhibitors, in collaboration with the European Lead Factory (Chapter 6). Using a primary surrogate substrate assay in combination with an orthogonal competitive ABPP assay, several novel serine hydrolase inhibitors were discovered. The 1,2,4-triazole sulfonamide ureas were selected for subsequent hit-to-lead optimization, resulting in a ~100 membered focused library. Assessment of the selectivity of this library with ABPP using probe MB064 identified several ABHD16A inhibitors. As aforementioned, MB064 efficiently visualizes ABHD16A activity, but also several additional serine hydrolases in mouse brain proteome, including DDHD domain containing 2 (DDHD2), ABHD6, ABHD12, and DAGL α .²¹ Hence MB064 was used to simultaneously assess activity on ABHD16A and selectivity over this panel of off-targets. Here the identification and optimization of potent 1,2,4-triazole sulfonamide urea ABHD16A inhibitors is described followed by *in vivo* characterization in mice.

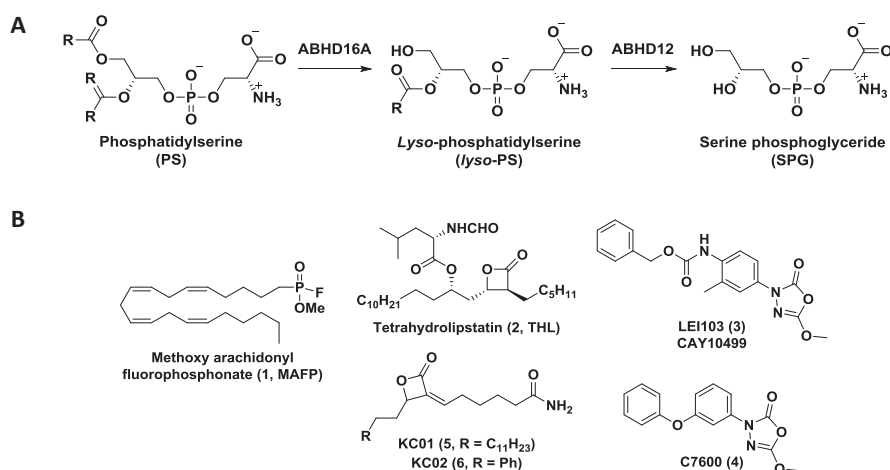


Figure 1. A) Phosphatidylserine (PS) and lyso-phosphatidylserine (lyso-PS) levels are regulated by α/β hydrolase domain type 12 and 16A (ABHD12 and ABHD16A). ABHD16A cleaves specifically at the PS *sn*-1 fatty ester, whereas ABHD12 cleaves the remaining *sn*-2 fatty ester of lyso-PS. **B)** Current inhibitors of ABHD16A are: *i*) Fluorophosphonates, such as methoxy arachidonoyl fluorophosphonate (**1**, MAFP), *ii*) β -Lactones (THL **2** and

KC01 **5**) and *iii*) 1,3,4-Oxadiazolones (LEI103, CAY10499 **3**) and C7600 (**4**). KC02 (**6**) has been reported as a paired inactive control compound of KC01 (**5**). Two activity-based probes (ABPs) have been reported for ABHD16A; TAMRA-fluorophosphonate (TAMRA-FP) and THL based β -lactone MB064.^{5,13,18,21}

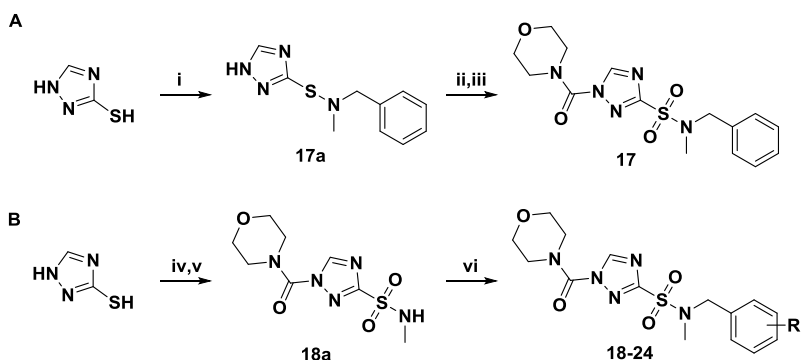
Results

Competitive ABPP on the focused library of 100 triazole sulfonamides (Chapter 6) revealed several 1,2,4-triazole sulfonamide ureas as ABHD16A inhibitors. All inhibitors, which have over 50% inhibitory effect on ABHD16A, are depicted in Table 1. Potency and selectivity of the inhibitors is influenced by the nature of the staying group (R_1 , compare **10** and **11**) as well as the leaving group (R_2 , compare **11-16**). ABHD16A seems to prefer small cyclic amine staying groups, since secondary and non-cyclic amines are not active (data not shown). The most potent ABHD16A inhibitors have, for example, a piperidine, morpholine or pyrrolidine as preferred staying group (entries **7**, **8** and **10**, Table 1). Of note, 3-phenyl substituted pyrrolidine is also allowed, indicating that a lipophilic pocket is present near the active site (entries **11-16**, Table 1). Compounds **14-16** show that triazole ureas sulfoxides are also allowed, albeit they appear to inhibit ABHD16A to a lesser extent. The leaving group can be enlarged, thereby increasing inhibitor potency (entries **14-16**, Table 1). This could indicate that the leaving group is located in a larger ABHD16A pocket.

All triazole ureas are non-selective and inhibit multiple off-targets (Table 1), which suggested that on one hand the triazole sulfonamide functions as a reactive warhead and on the other hand that the enzymes share similar active sites in which the current substituents are not able to make selective interactions. Increasing potency and selectivity are, therefore, the two main priorities for the hit-to-lead optimization process. Compound **8** appeared the most selective inhibitor based on a single concentration (Table 1). Therefore compound **8** was profiled in a full dose response using competitive ABPP with MB064 on mouse membrane proteome (Figure 2). Compound **8** had an IC_{50} of ~ 400 nM on ABHD16A and did not inhibit DAGL α . ABHD6 and ABHD12 were identified as important off-target activities. To study *lyso*-PS formation, it will be important to have inhibitors which are selective over ABHD12. Compound **10**, a methyl substituted sulfonamide, does not exhibit any ABHD12 activity, therefore it was decided to investigate the effect of methylation of the sulfonamide in compound **8**. To this end, a synthetic route was developed as depicted in Scheme 1A. In brief, sulfenamide **17a** was obtained from *in situ* prepared *N*-chloro-*N*-methylbenzylamine and subsequently treated with morpholine carbamoyl chloride. Lastly sulfonamide **17** was synthesized from the corresponding sulfenamide by oxidation with $NaIO_4$ and $RuCl_3$.

Table 1. Initial hit compounds for ABHD16A, sulfonamides **7-13** and sulfoxides **14-16**. R¹ is staying group, R² is leaving group. Values are % inhibition in ABPP for ABHD6, 12, 16, DDHD2 and FAAH, at 10 μM inhibitor concentration (N = 1). DAGLα values are pIC₅₀ PNP assay in dose response analysis (N = 2, n = 2). See experimental section for assay procedures.

#	R ¹	R ²	ABHD16A (% eff.)	ABHD12 (% eff.)	DDHD2 (% eff.)	ABHD6 (% eff.)	FAAH (% eff.)	DAGLα PNP (pIC ₅₀)
7			100	56	99	96	84	6.1
8			100	83	0	94	73	< 4.7
9			74	86	70	99	51	7.2
10			91	0	73	98	98	6.3
11			76	50	100	99	100	7.2
12			72	38	87	95	100	8.0
13			59	53	96	99	98	7.1
14			52	0	94	94	90	7.0
15			64	57	84	99	98	7.9
16			78	73	100	92	100	8.0



Scheme 1. Synthesis of 1,2,4-triazole sulfonamides **17-24**. A) Initial synthesis of compound **17**: *i*) NCS, NMeBn 0°C, CH₂Cl₂, 30 min, then 1,2,4-triazole-3-thiol (sol. in THF), rt, 3h. *ii*) Morpholine carbamoyl chloride, DIPEA, DMAP, rt, 10 h. 16% (2 steps). *iii*) NaI, RuCl₃, MeCN/H₂O 3:1, rt, 14 h., 43% (**17**). B) Synthesis of compounds **18-24**

24, with last step derivatization of R-group: *iv*) NaOCl, HCl, H₂O, Dioxane, DCM, then NHMe (aq), rt, 2 hr. *v*) Morpholine carbamoyl chloride, DIPEA, DMAP, rt, ON, 28% yield over 2 steps. *vi*) Derivatization; corresponding benzyl/ phenoxybenzyl halide, NaH, rt, ON, 3-50% yield. R = H, 4-Me, 4-Cl, 4-OMe, 4-OPh, 3-OPh, 3(2-oxy-5-(trifluoromethyl)pyridine) (**18-24**).

Dose response analysis of **17** on ABPP indicated that it was a potent ABHD16A inhibitor with an IC₅₀ of 616 nM and 100-fold selectivity over ABHD12 (Figure 2). However, off-target ABHD6 activity was significantly increased.

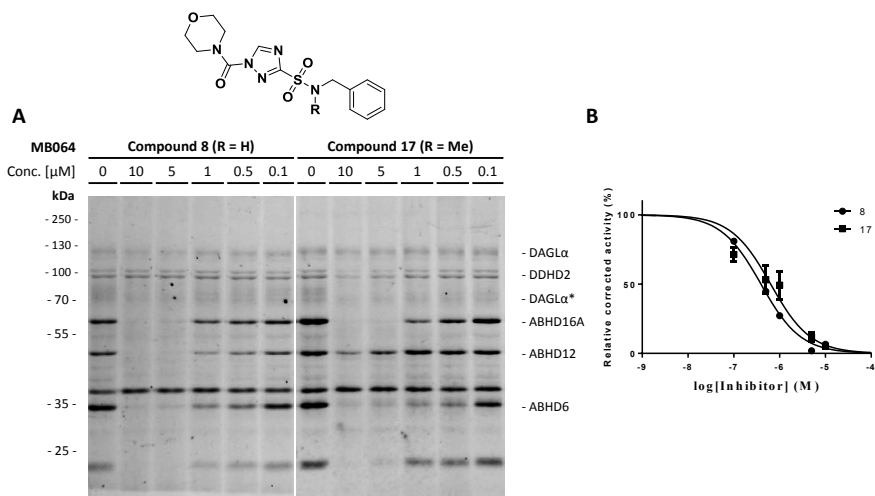
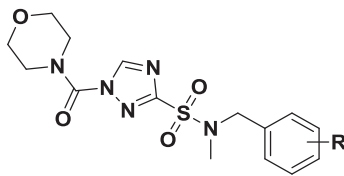


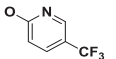
Figure 2. **A**) On-gel dose response analysis of hit compound **8** (R = H) and optimized compound **17** (R = Me) on ABPP with MB064 on mouse brain proteome. Compound **8** competes with probe labeling on ABHD16A, as well as ABHD6 and ABHD12. Compound **17** competes with probe labeling on ABHD16A with equal potency compared to **8**, but displays some ~100 fold more selectivity over ABHD12. **B**) Dose response curve of compounds **8** (N = 1) and **17** (N = 3). pIC₅₀ values: 6.41 and 6.18 \pm 0.18 (for compounds **8** and **17** respectively).

An optimization strategy, analogous to a Topliss scheme, was conducted on the benzylamine group of compound **17**, in which a *p*-methyl group (**18**), an electron withdrawing (*p*-Cl, **19**) or donating substituent (*p*-OMe, **20**) were introduced to investigate the electronic and lipophilic properties of the phenyl ring (see Scheme 1B for the synthetic route). Compound **19** showed increased inhibitor potency, whereas **20** was equally active and **18** was less active (4-Cl > 4-OMe > H > 4-Me, Table 2, entries **17-20**). Of note, preference for electron withdrawing and lipophilic substituents has also been observed during optimization of 1,3,4-oxadiazol-2(3*H*)-ones C7600 as ABHD16A inhibitors.¹³ To probe the size of the binding pocket, a 4-phenoxy moiety was introduced (**21**). This increased inhibitor potency almost 33-fold compared to **17** (Table 2). Similar to the development of C7600 (Figure 1),¹³ changing the phenoxy substituent from *para*- to *meta*-position (**22**) increased inhibitor potency, almost 100-fold compared to compound **17** (Table 2). This suggests that the aryl ether substituent is located in a lipophilic pocket that normally accommodates an acyl chain of PS. Lastly, compound **23** was designed, in which the biphenyl ether was replaced by a 3-(2-

pyridinyl)-4-CF₃ phenoxy ether. This group has been previously applied in PF-04457845, a clinical trial drug candidate for another serine hydrolase FAAH, to increase metabolic stability.²² The activity of compound **23** was, however, slightly decreased (Table 2), which could perhaps be explained by its reduced lipophilicity.

Table 2. Structure-activity relationships of 1,2,4-triazole sulfonamides **17-23** as ABHD16A inhibitors. Activity assay is ABPP on mouse brain. Values are ABHD16A pIC₅₀ ± SEM, N = 3. pIC₅₀ values were determined using Graphpad Prism after normalization to control and correction for protein loading via Coomassie staining. The activity-based probe is MB064 (250 nM final concentration).



Entry	R group	R position	pIC ₅₀ ± SEM
17	H	-	6.18 ± 0.18
18	Me	4	5.02 ± 0.16
19	Cl	4	7.48 ± 0.04
20	OMe	4	6.84 ± 0.13
21	OPh	4	7.70 ± 0.20
22	OPh	3	8.10 ± 0.13
23		3	7.44 ± 0.27

To obtain a more comprehensive selectivity profile of compounds **22** and **23**, a comparative ABPP assay was performed using two ABPs, *i.e.* MB064 and TAMRA-FP (Figure 3). Both compounds were not selective and did inhibit several serine hydrolases. ABHD6 was identified as an important off-target. Moreover, inhibition of DDHD2, ABHD12 and FAAH is observed at the highest inhibitor concentrations for both **22** and **23**. Compound **22** appeared more fold-selective due to its higher potency on ABHD16A in the ABPP setting (Table 3).

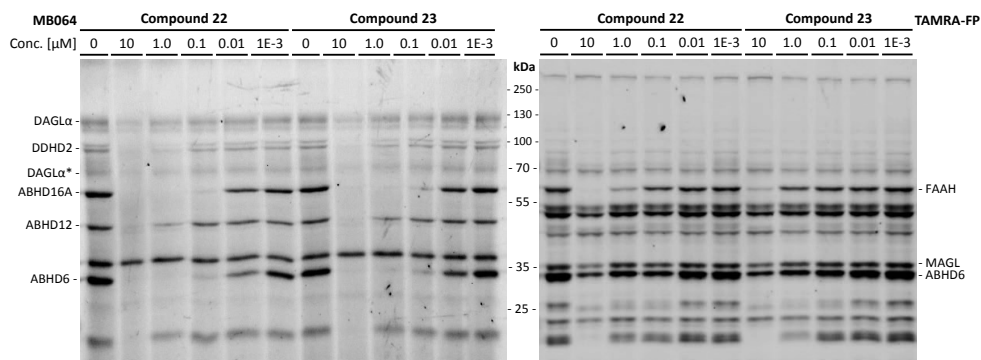


Figure 3. Representative gels of the selectivity profile of compounds **22** and **23** on mouse brain proteome using ABPs MB064 and TAMRA-FP. Both compounds were measured at N = 3.

Table 3. All identified and quantified off-targets of **22** and **23** in mouse brain proteome. N = 3. pIC_{50} values were determined using Graphpad Prism after normalization to control and correction for protein loading via Coomassie staining. All values are N = 3. The activity-based probe is MB064 (250 nM final concentration) and TAMRA-FP (500 nM final concentration). Apparent selectivity is determined as $IC_{50}/IC_{50}(\text{ABHD16A})$.

	$pIC_{50} \pm SEM$ 22	Apparent fold selectivity	$pIC_{50} \pm SEM$ 23	Apparent fold selectivity
ABHD16a	8.10 ± 0.13	-	7.44 ± 0.27	-
DAGLα	5.46 ± 0.11	437	5.15 ± 0.20	195
DDHD2	6.75 ± 0.30	22	6.52 ± 0.20	8
ABHD12	6.29 ± 0.20	65	6.07 ± 0.12	23
ABHD6	8.18 ± 0.08	1	7.70 ± 0.10	1
LyPLA1/2	5.86 ± 0.10	174	5.62 ± 0.16	66
FAAH	6.14 ± 0.10	91	5.68 ± 0.10	58
PLA2G7	4.64 ± 0.18	>1000	4.62 ± 0.14	661
MAGL	4.97 ± 0.07	>1000	4.88 ± 0.08	363

Next, the activity of both compounds was measured on recombinant human ABHD16A overexpressed in HEK293T cell membrane fractions. Active hABHD16A was labelled by MB064 and dose dependently competed by **22** and **23**. The pIC_{50} s were 7.67 ± 0.13 and 7.54 ± 0.11 for **22** and **23**, respectively (N = 3, Figure 4A). To assess whether **22** and **23** were active in a cellular setting, an *in situ* ABHD16A cellular assay was developed using Neuro 2A cells (N2A) that endogenously express ABHD16A. Compound **22** was highly active on ABHD16A, as 5 minutes pre-incubation of living N2A cells with 100 nM of **22** completely

blocked ABHD16A labeling by MB064 (Figure 4B, panel 1). Surprisingly, ABHD6 was not significantly inhibited, even at the highest incubation time tested (60 min with 100 nM of **16**, Figure 4B, panel 1). ABHD16A has an extracellular localization whereas ABHD6 has not, indicating that **22** and **23** cannot cross the cell membrane effectively. Upon further investigation, both compounds dose-dependently blocked ABHD16A labeling by ABP MB064 (Figure 4B). Similar cellular activity was observed for both compounds ($pIC_{50} = 7.8 \pm 0.1$ and 7.9 ± 0.1 for **22** and **23**, respectively). Of note, an unidentified off-target (Figure 4B, * in panels 1-3) was observed in N2A cells.

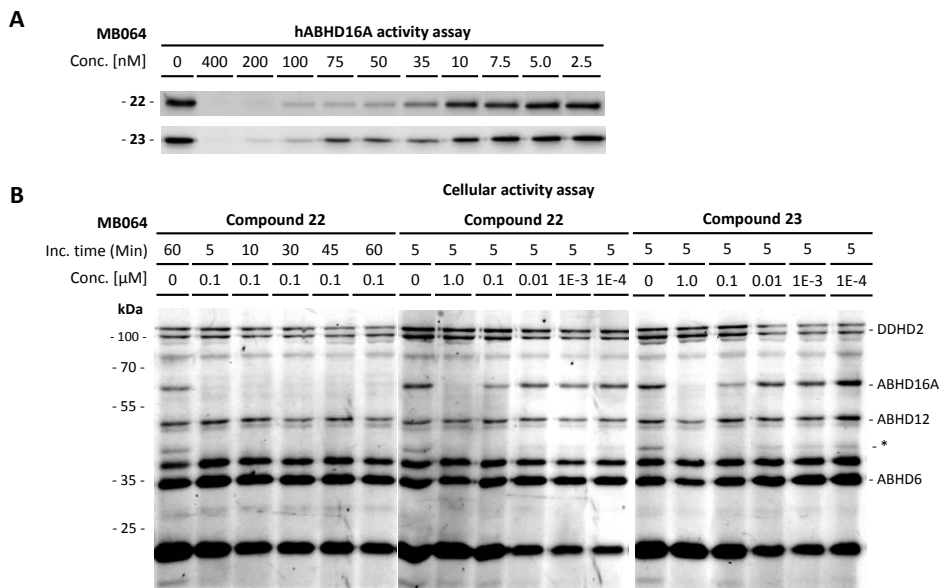


Figure 4. A) Dose response analysis of **22** and **23** on human ABHD16A overexpressed HEK293T cell membrane fractions. pIC_{50} values are 7.67 ± 0.13 and 7.54 ± 0.11 for **22** and **23**, respectively. **B)** Cellular Neuro 2A assay. Panel 1; Time dependent incubation of compound **22** at 100 nM concentration. Labeling of cellular ABHD16A is completely prevented at 5 minutes incubation with compound **22**. Panel 2; *In situ* dose response analysis of compound **22** on cellular ABHD16A with 5 minutes pre-incubation. Panel 3; *In situ* dose response analysis of compound **23** on cellular ABHD16A. $pIC_{50} = 7.8 \pm 0.1$ and 7.9 ± 0.1 for **22** and **23** respectively. * is an off-target of **22** and **23** which remains to be identified. pIC_{50} values were determined using Graphpad Prism after normalization to control and correction for protein loading via Coomassie staining. All values are N = 3. The activity-based probe is MB064 (250 nM final concentration).

Finally, it was investigated if both compounds would be able to inhibit ABHD16A activity *in vivo*. 12 Male C57 black-6 mice were divided into 4 groups, 3 mice served as control, and the remaining mice received either 45 mg/kg or 15 mg/kg of compound **22**, or 45 mg/kg of compound **23** by *i.p.* injection. The mice appeared to exhibit normal behaviour after administration of the compounds. After two hours, the mice were sacrificed by cervical dislocation. Brain and spleen tissues were harvested, lysed and subjected to ABPP analysis using ABPs MB064 and TAMRA-FP. Both compounds significantly reduced ABHD16A labeling

by MB064 in brain (Figure 5), albeit not fully at the highest dose tested. This indicates that the compounds are active *in vivo*, but may have difficulties crossing the blood brain barrier (BBB). This hypothesis is strengthened by analysis of mouse spleen, here multiple proteins are fully inhibited (see supporting information). Interestingly, both compounds did not seem to inhibit brain ABHD6 to a large extent (Figure 5A, panel 1), which is in line with the results obtained from the cellular experiments and indicates restricted cell permeability. ABHD12 and ABHD6 do appear to be inhibited to a minor extent. The reduced DAGL α labeling is probably an artefact, as this enzyme is very sensitive towards degradation due to freeze-thaw cycles. Labeling by broad-spectrum probe TAMRA-FP displays some minor inhibition on FAAH and MAGL (Figure 5A, panel 2) at the highest dose tested.

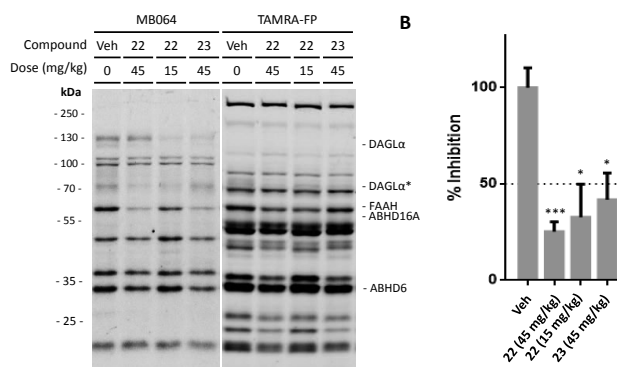


Figure 5. A) Representative gels of the *in vivo* characterization of compounds **22** and **23** with ABP MB064 and TAMRA-FP on mouse brain. Significant reduction of ABHD16A labeling is observed. Some reduced DAGL α labeling is also observed, which is due to instability of this enzyme. **B)** Average inhibition of ABHD16A MB064 labeling in brain by compounds **22** and **23** (N = 3). Significance, T-Test: *P < 0.05; **P < 0.01; ***P < 0.001.

Conclusions

To conclude, 1,2,4-triazole sulfonamides were discovered as potent ABHD16A inhibitors. Original hit compound **8**, was rapidly optimized to **22** and **23** using a rational design approach. Both compounds were active on murine as well as human ABHD16A and were active in a cellular context. Cellular experiments strongly indicate that both compounds do not penetrate cells efficiently, but do potently inhibit extracellular ABHD16A. 1,2,4 Triazole sulfonamides **22** and **23** partially, but significantly, inhibit ABHD16A *in vivo*, after *i.p.* administration. This makes compounds **22** and **23**, the first *in vivo* active ABHD16A inhibitors in current literature. As brain ABHD16A was not completely inhibited at high doses of both compounds, future work could focus on optimization of brain penetration by decreasing the polar surface area and increasing metabolic stability. This optimization, however, is highly likely to increase off-target activity *in vivo*. Hence the development of a paired inactive control compound is advised, to exclude potential off-targets effect during studies on animal

models. The structure-activity relationships from this study provide an excellent starting point for further optimization of the next generation of *in vivo* active ABHD16A inhibitors. Ultimately it is shown that 1,2,4-triazole sulfonamides may provide excellent tool compounds to investigate the role of ABHD16A inhibition as a potential treatment of the debilitating disease PHARC.

Experimental

Procedures chemical biology

Cell Culture and Membrane Preparation

Cell culture and membrane preparations were performed as earlier reported.¹⁹ In brief, HEK293T and N2A cells were grown in DMEM with stable glutamine and phenol red (PAA or Sigma) with 10% new born calf serum, penicillin, and streptomycin. Cells were passaged every 2–3 days by resuspension in medium and seeding to the appropriate confluence.

Membranes were prepared from transiently transfected HEK293T. One day prior to transfection, 10^7 cells were seeded in a 15 cm Petri dish. Cells were transfected by the addition of a 3:1 mixture of polyethyleneimine (60 μ g) and plasmid DNA (20 μ g) in 2 mL of serum free medium. The medium was refreshed after 24 h, and after 72 h the cells were harvested by suspending them in 20 mL of medium. The suspension was centrifuged for 10 min at 1000 rpm, and the supernatant was removed. The cell pellet was stored at -80°C until use.

Cell pellets were thawed on ice and suspended in lysis buffer A (20mM HEPES, pH 7.2, 2 mM DTT, 0.25 M sucrose, 1 mM MgCl_2 , 25 U/mL Benzonase). For hABHD16a HEK293T membrane preparations, protease inhibitor cocktail was not added. The suspension was homogenized by polytrone (3×7 s) and incubated for 30 min on ice. The suspension was subjected to ultracentrifugation (93,000g, 30 min, 4°C , Beckman Coulter, type Ti70 rotor) to yield the cytosolic fraction in the supernatant and the membrane fraction as a pellet. The pellet was suspended in lysis buffer B (20 mM HEPES, pH 7.2, 2 mM DTT). The protein concentration was determined with a Quick Start Bradford assay (Biorad). The protein fractions were diluted to a total protein concentration of 5 and 9 mg/mL and stored in aliquots at -80°C until use.

Colorimetric DAG α assay (PNP-butyrate assay)

The colorimetric DAG α activity assay was performed as previously reported.^{19,21,23,24}

Tissue sample preparation

Tissue sample preparations was performed as earlier reported.¹⁹ In brief, mouse brains were isolated according to guidelines approved by the ethical committee of Leiden University (DEC#14137). Mouse brains were thawed on ice and dounce-homogenized in lysis buffer A (20 mM HEPES, 2 mM DTT, 1 mM MgCl_2 , 25 U/mL Benzonase) and incubated for 15 minutes on ice, followed by low speed spin (2500 \times g, 3 min. at 4°C) to remove debris. The supernatant was subjected to ultracentrifugation (37,000 rpm, 45 min. 4°C , Beckman Coulter, Type Ti70 rotor) to yield the cytosolic fraction in the supernatant and the membrane fraction as a pellet. The pellet was resuspended in lysis buffer B (20 mM HEPES, 2 mM DTT). The total protein concentration was determined with Quick Start Bradford assay (Biorad). Membranes were stored in small aliquots at -80°C until use.

Cellular ABPP experiment

Neuro2A (N2A) cells were grown according to the cell culture protocol above. Cells were harvested, homogenized by pipetting and washed 3x with serum free DMEM medium. The cells were divided equally over 6-well cell culture plates and stabilized for 30 min at 37°C . Inhibitors were added from the corresponding DMSO stock (1:1000 final DMSO conc.) to the appropriate inhibitor conc. (1.0 μM – 0.1 nM). Cells were incubated for the appropriate time (5-60 min.) with inhibitor and after washed 3 x with PBS and harvested in

PBS. The samples were centrifuged in eps for 10 min at 8000 rpm, the supernatant was removed and the samples were flash frozen in liquid nitrogen.

The cell pellets were thawed on ice, lysis buffer A (20 mM HEPES, 2 mM DTT, 1 mM MgCl₂, 25 U/mL Benzonase) was added, whereafter the samples were mixed with a pipet and incubated for 15 minutes on ice. Protein concentration of all the samples was determined with a Bradford assay. Samples were diluted to 2 mg/ mL with lysis buffer B (20 mM HEPES, 2 mM DTT) and analysed using the ABPP protocol as previously reported and described below.¹⁹

ABPP for murine and human ABHD16A

ABPP was performed as earlier reported.¹⁹ In brief, IC₅₀ determination of inhibitors against endogenously expressed ABHD16A in the mouse brain membrane proteome. Inhibitors were incubated at the indicated concentrations (total volume 20 µL) for 30 min at rt, prior to incubation with probe MB064 or TAMRA-FP for 15 min at rt. The reaction was quenched with 7.5 µL standard 4 × SDS page sample buffer, and resolved on 10 % SDS-page. The gels were scanned and the percentage activity remaining was determined by measuring the integrated optical intensity of the bands using Image Lab 5.2. software. IC₅₀ values were determined from a dose-response curve generated using Prism software (GraphPad).

ABPP of *in vivo* samples

ABPP was performed as earlier reported.¹⁹ In brief, proteomes were diluted to the same concentration (Brain = 2 mg/ mL, Testis = 1mg/ mL, Spleen = 0.5 mg/mL) and 20 µL of proteome incubated with either MB064 (final concentration: 250 nM) or TAMRA-FP (Thermo Fischer Scientific, final concentration: 500nM) at rt for 15 minutes. The reactions were quenched using 7.5 µL of standard SDS-PAGE sample buffer. The samples were then directly loaded and resolved on SDS-PAGE gels (10% acrylamide). The gels were scanned using a ChemiDoc MP system and analysed using ImageLab v.4.1. IC₅₀ values were determined by integration of the fluorescent proteins bands, corrected for protein loading using Coomassie staining, and expression of the band intensity relative to control (DMSO). The resultant data were then exported to Graphpad Prism v.5 and analysed using non-linear fitting. All values are based on N = 3, and SEMs are given for each data point.

In vivo dosing experiments

Compounds **22** and **23** were prepared as a solution or emulsion in carrier, consisting of 18:1:1 PBS:PEG-40:EtOH. The final concentrations of the solution were 1.5 mg/µL and 4.5 mg/µL. Twelve C57 Black-6 (C57BL/6) mice, 10-weeks of age, were weighted prior to intraperitoneal (i.p) injection of the compounds at 15 mg/kg and 45 mg/kg dosing respectively (1 µL/ kg). Mice receiving only carrier served as the control group (3 mice per group). After 2 hours the mice were sacrificed by cervical dislocation, the tissues harvested and immediately flash frozen in liquid nitrogen (DEC#14137, Date of experiment: 08-12-'15).

Procedures chemistry

General Remarks.

All reactions were performed using oven- or flame-dried glassware and dry solvents. Reagents were purchased from Sigma-Aldrich, Acros, and Merck and used without further purification unless noted otherwise. All moisture sensitive reactions were performed under an argon atmosphere. Traces of water were removed from starting compounds by coevaporation with toluene. ¹H and ¹³C NMR spectra were recorded on a Bruker AV 400 MHz spectrometer at 400.2 (¹H) and 100.6 (¹³C) MHz using the reported deuterated solvent. Chemical shift values are reported in ppm with tetramethylsilane or solvent resonance as the internal standard (CDCl₃: δ 7.26 for ¹H, δ 77.16 for ¹³C; CD₃OD: δ 3.31 for ¹H, δ 49.00 for ¹³C; CD₃CN: δ 1.94 for ¹H, δ 118.32 and 1.32 for ¹³C). Data are reported as follows: chemical shifts (δ), multiplicity (s = singlet, d = doublet, dd = double doublet, td =

triple doublet, t = triplet, q = quartet, quintet = quint, b = broad, m = multiplet, appd = apparent doublet), coupling constants J (Hz), and integration. High resolution mass spectra were recorded on a Thermo Scientific LTQ Orbitrap XL. Compound purity was measured by liquid chromatography on a Finnigan Surveyor LC-MS system equipped with a C18 column. Flash chromatography was performed using SiliCycle silica gel type SiliaFlash P60 (230–400 mesh). TLC analysis was performed on Merck silica gel 60/Kieselguhr F254, 0.25 mm. Compounds were visualized using either a KMnO_4 -stain (K_2CO_3 (40 g), KMnO_4 (6 g), and H_2O (600 mL)) or Ninhydrin-stain (Ninhydrin (200mg), *n*-butanol (95ml) and AcOH (10%, 5ml)).

***N*-Methyl-*N*-phenyl-1-(piperidine-1-carbonyl)-1*H*-1,2,4-triazole-3-sulfonamide (7)**

Verified screening hit. HRMS (ESI+) m/z : calculated for $\text{C}_{15}\text{H}_{20}\text{N}_5\text{O}_4\text{S}$ ([M + H]), 350.1281; found, 350.1283. Purity of >95% as determined by LC-MS.

***N*-Benzyl-1-(morpholine-4-carbonyl)-1*H*-1,2,4-triazole-3-sulfonamide (8)**

Verified screening hit. HRMS (ESI+) m/z : calculated for $\text{C}_{14}\text{H}_{18}\text{N}_5\text{O}_4\text{S}$ ([M + H]), 352.1074; found, 352.1068. Purity of >95% as determined by LC-MS.

***N*-Benzyl-*N*-methyl-1-(pyrrolidine-1-carbonyl)-1*H*-1,2,4-triazole-3-sulfonamide (10)**

Verified screening hit. HRMS (ESI+) m/z : calculated for $\text{C}_{15}\text{H}_{20}\text{N}_5\text{O}_3\text{S}$ ([M + H]), 350.1281; found, 350.1283. Purity of >95% as determined by LC-MS.

***N*-Benzyl-*N*-methyl-1-(3-phenylpyrrolidine-1-carbonyl)-1*H*-1,2,4-triazole-3-sulfonamide (11)**

Verified screening hit. HRMS (ESI+) m/z : calculated for $\text{C}_{21}\text{H}_{24}\text{N}_5\text{O}_3\text{S}$ ([M + H]), 426.1594; found, 426.1592. Purity of >95% as determined by LC-MS.

3-((Benzyl(methyl)amino)thio)-1*H*-1,2,4-triazol-1-yl)(morpholino)methanone (17a)

To a stirred solution of *N*-chlorosuccinimide (3.3 g, 25 mmol) in CH_2Cl_2 (80 mL) was slowly added methylbenzylamine (9.6 mL, 75 mmol) at 0°C. After 30 minutes a solution of commercially available 1,2,4-triazole-3-thiol (2.5 g, 25 mmol) in dry THF (60 mL) was added slowly and the solution was gradually warmed up to rt and was stirred for an additional 3 h. The reaction mixture was poured into acetone, filtered, concentrated *in vacuo* and purified by flash chromatography. The sulfenamide was dissolved in dry THF (10 mL) and cooled to 0°C, after which was added DIPEA (262 μL , 1.5 mmol) and DMAP (12.2 mg, 0.1 mmol) and finally morpholinecarbonyl chloride (133.5 μL , 1.1 mmol). The mixture was stirred for 4h until completion, after which the reaction mixture was diluted with EtOAc, washed with water, brine, dried, concentrated *in vacuo* and purified by flash chromatography to obtain 3-((benzyl(methyl)amino)thio)-1*H*-1,2,4-triazol-1-yl)(morpholino)methanone (53 mg, 0.16 mmol, 16%). ^1H NMR (CD_3CN , 400 MHz): δ 8.77 (s, 1H), 7.35-7.27 (m, 5H), 4.27 (s, 2H), 3.78 (brs, 4H), 3.74 (s, 4H), 2.93 (s, 3H). ^{13}C NMR (CD_3CN , 101 MHz): δ 163.99, 149.30, 148.38, 139.43, 129.86(2C), 129.28(2C), 128.47, 67.09(2C), 64.94, 47.52(2C), 46.40.

***N*-benzyl-*N*-methyl-1-(morpholine-4-carbonyl)-1*H*-1,2,4-triazole-3-sulfonamide (17)**

To a stirred solution of 3-((benzyl(methyl)amino)thio)-1*H*-1,2,4-triazol-1-yl)(morpholino)methanone (**17a**, 10 mg, 30 nmol) in MeCN/ H_2O (3:1) was added NaIO_4 (19.3 mg, 90 nmol, 3 eq) and RuCl_3 (0.5 mg, 2.4nmol, 0.08 eq). The solution was stirred at rt for 14 h. until completion, after which the reaction mixture was diluted with EtOAc, washed with water, brine, dried, concentrated *in vacuo* and purified by flash chromatography to obtain *N*-benzyl-*N*-methyl-1-(morpholine-4-carbonyl)-1*H*-1,2,4-triazole-3-sulfonamide (4.3 mg, 13 nmol, 43%). HRMS (ESI+) m/z : calculated for $\text{C}_{15}\text{H}_{20}\text{N}_5\text{O}_4\text{S}$ ([M + H]), 366.1231; found, 366.1229. ^1H NMR (400 MHz, CDCl_3) δ 8.88 (s, 1H), 7.41 – 7.29 (m, 5H), 4.45 (s, 2H), 3.81 (s, 8H), 2.87 (s, 3H). ^{13}C NMR (101 MHz, CDCl_3) δ 148.19, 147.48,

141.90, 135.15, 129.13, 128.89, 128.53(2C), 128.31(2C), 66.62, 54.74, 47.92, 34.97. Purity of 93% as determined by LC-MS.

***N*-methyl-1-(morpholine-4-carbonyl)-1*H*-1,2,4-triazole-3-sulfonamide (18a)**

To a cooled (-10°C) stirred solution of HCl in dioxane (4 M, 16 mL, 120 mmol) was added dry CH₂Cl₂ (80 mL) and subsequently aq. NaOCl solution (10%, 25 mL, 120 mmol) was added dropwise. After 15 minutes of stirring, 1,2,4-triazole-3-thiol (0.5 g, 5 mmol) was added and the solution was stirred for an additional 30 minutes and quenched with aqueous methylamine (11 M, 5 mL, 55 mmol). The solution was allowed to gradually warm up to rt, stirred for an additional 2 hours and subsequently concentrated *in vacuo*. The residue was taken up dry THF (80 mL) after which was added DIPEA (1.3 mL, 75 mmol), DMAP (60 mg, 0.5 mmol) and morpholine carbamoyl chloride (0.88 mL, 7.5 mmol). The solution was stirred at rt for 14 h. until completion, after which the reaction mixture was concentrated *in vacuo* and purified by flash chromatography to obtain *N*-methyl-1-(morpholine-4-carbonyl)-1*H*-1,2,4-triazole-3-sulfonamide (385 mg, 1.4 mmol, 28%). ¹H NMR (400 MHz, CD₃CN) 8.87 (s, 1H), 5.95 (d, *J* = 3.60Hz, 1H), 3.72 (s, 8H), 2.73 (d, *J* = 5.2Hz, 3H). ¹³C NMR (101 MHz, CD₃CN) δ 162.33, 149.22, 148.60, 66.94 (2C), 47.51 (brs, 2C), 29.90.

***N*-methyl-*N*-(4-methylbenzyl)-1-(morpholine-4-carbonyl)-1*H*-1,2,4-triazole-3-sulfonamide (18)**

To a stirred solution of NaH (11 mg, 0.27 mmol, 60% in mineral oil) in dry DMF was added *N*-methyl-1-(morpholine-4-carbonyl)-1*H*-1,2,4-triazole-3-sulfonamide (**18a**, 74 mg, 0.27 mmol) and commercially available 4-methylbenzyl bromide (50 mg, 0.27 mmol). The solution was stirred for 14 hours until completion, after which the reaction mixture was diluted with EtOAc, washed with brine 3x, dried, concentrated *in vacuo* and purified by flash chromatography to obtain *N*-methyl-*N*-(4-methylbenzyl)-1-(morpholine-4-carbonyl)-1*H*-1,2,4-triazole-3-sulfonamide (52 mg, 0.14 mmol, 50%). LC-MS (ESI+) *m/z*: calculated for C₁₆H₂₂N₅O₄S ([M + H]), 380.14; found, 379.73. ¹H NMR (400 MHz, CD₃CN) δ 8.89 (s, 1H), 7.24 - 7.16 (m, 4H), 4.34 (s, 2H), 3.72 (bs, 8H), 2.81 (s, 3H), 2.32 (s, 3H). ¹³C NMR (101 MHz, CD₃CN) δ 161.78, 149.22, 148.59, 138.77, 133.68, 130.23(2C), 129.32(2C), 66.96(2C), 54.86, 47.70(bs, 2C), 35.54, 21.15. Purity of 90% as determined by LC-MS.

***N*-(4-chlorobenzyl)-*N*-methyl-1-(morpholine-4-carbonyl)-1*H*-1,2,4-triazole-3-sulfonamide (19)**

The title compound was synthesized from *N*-methyl-1-(morpholine-4-carbonyl)-1*H*-1,2,4-triazole-3-sulfonamide (**18a**, 100 mg, 0.36 mmol) and commercially available 4-chlorobenzyl chloride (58 mg, 0.36 mmol) according to procedure described for compound **12**. This yielded *N*-(4-chlorobenzyl)-*N*-methyl-1-(morpholine-4-carbonyl)-1*H*-1,2,4-triazole-3-sulfonamide (12 mg, 0.03 mmol, 9%) after preparative HPLC purification. HRMS (ESI+) *m/z*: calculated for C₁₅H₁₉ClN₅O₄S ([M + H]), 400.0841; found, 400.0837. ¹H NMR (400 MHz, CDCl₃) δ 8.89 (s, 1H), 7.36 - 7.28 (m, 4H), 4.42 (s, 2H), 4.12 - 3.68 (m, 8H), 2.86 (s, 3H). ¹³C NMR (101 MHz, CDCl₃) δ 161.65, 148.22, 147.40, 134.21, 133.75, 129.82(2C), 129.08(2C), 66.56(2C), 54.11, 48.1(bs), 45.94(bs), 35.00. Purity of 97% as determined by LC-MS.

***N*-(4-methoxybenzyl)-*N*-methyl-1-(morpholine-4-carbonyl)-1*H*-1,2,4-triazole-3-sulfonamide (20)**

The title compound was synthesized from *N*-methyl-1-(morpholine-4-carbonyl)-1*H*-1,2,4-triazole-3-sulfonamide (**18a**, 68 mg, 0.25 mmol) and commercially available 4-methoxybenzyl chloride (37 μL, 0.25 mmol) according to procedure described for compound **12**. This yielded *N*-(4-methoxybenzyl)-*N*-methyl-1-(morpholine-4-carbonyl)-1*H*-1,2,4-triazole-3-sulfonamide (26 mg, 0.1 mmol, 40%). HRMS (ESI+) *m/z*: calculated for C₁₆H₂₂N₅O₅S ([M + H]), 396.1336; found, 396.1334. ¹H NMR (400 MHz, CD₃CN) δ 8.89 (s, 1H), 7.25 (d, *J* = 8.8 Hz, 2H), 6.90 (d, *J* = 8.8 Hz, 2H), 4.32 (s, 2H), 3.77 (s, 3H), 3.71 (brs, 8H), 2.80 (s, 3H). ¹³C NMR (101 MHz, CD₃CN) δ 161.84, 160.48, 149.21, 148.60, 130.80(2C), 128.53, 114.93(2C), 66.96(2C), 55.92, 54.57, 47.52 (brs, 2C), 35.43. Purity of 90% as determined by LC-MS.

4-Phenoxybenzyl alcohol (24)

To a stirred solution of commercially available 4-phenoxybenzaldehyde (1.0 g, 5.0 mmol) in dry THF (40 mL) was added borane in THF (6.0 mL, 1 M, 6 mmol) at 0°C. The reaction was stirred for 10 minutes and was then allowed to warm up to rt. The solution was stirred for 1 h. until completion, after which was added 10 mL of sat. NH₄Cl (aq.). The mixture was diluted with EtOAc (40 mL), washed with brine, dried, filtered, concentrated *in vacuo* to obtain 4-phenoxybenzyl alcohol (0.99 g, 4.9 mmol, 99%). ¹H NMR (400 MHz, CDCl₃) δ 7.35-7.31 (m, H), 7.10 (t, *J* = 7.4 Hz, H), 7.01-6.99 (m, H), 4.67 (s, 2H), 1.78 (brs, 1H). ¹³C NMR (101 MHz, CDCl₃) δ 157.31, 156.94, 135.85, 129.89(2C), 128.83(2C), 123.43, 119.08(2C), 118.99(2C), 65.04.

4-Phenoxybenzyl bromide (25)

To a stirred solution of 4-phenoxybenzyl alcohol (**24**, 0.99 g, 4.94 mmol) in dry CH₂Cl₂ (40 mL) was added 33% HBr in HOAc (10 mL) at 0°C. The reaction was stirred for 10 minutes and was then allowed to warm up to rt. The solution was stirred for 14 h. until completion, after which was added 20 mL of sat. NaHCO₃ (aq.). The mixture was extracted with CH₂Cl₂ (3 x 40 mL), washed with brine, dried, filtered, concentrated *in vacuo* to obtain 4-phenoxybenzyl bromide (821 mg, 4.10 mmol, 83%). ¹H NMR (400 MHz, CDCl₃) δ 7.34-7.30 (m, 4H), 7.10 (t, *J* = 7.2 Hz, 1H), 7.00 (d, *J* = 8.2 Hz, 2H), 6.93 (d, *J* = 8.8 Hz, 2H), 4.46 (s, 2H).

***N*-methyl-1-(morpholine-4-carbonyl)-*N*-(4-phenoxybenzyl)-1*H*-1,2,4-triazole-3-sulfonamide (21)**

The title compound was synthesized from *N*-methyl-1-(morpholine-4-carbonyl)-1*H*-1,2,4-triazole-3-sulfonamide (**18a**, 281 mg, 1.02 mmol) and 4-phenoxybenzyl bromide (**25**, 253 mg, 0.96 mmol) according to procedure described for compound **18**. This yielded *N*-methyl-1-(morpholine-4-carbonyl)-*N*-(4-phenoxybenzyl)-1*H*-1,2,4-triazole-3-sulfonamide (24 mg, 0.05 mmol, 5%). HRMS (ESI+) *m/z*: calculated for C₂₁H₂₄N₅O₅S ([M + H]), 458.1493; found, 458.1492. ¹H NMR (400 MHz, CD₃CN) δ 8.90 (s, 1H), 7.41-7.32 (m, 4H), 7.16 (t, *J* = 7.2 Hz, 1H), 7.03- 6.97 (m, 4H), 4.37 (s, 2H), 3.72 (brs, 8H), 2.84 (s, 3H). ¹³C NMR (101 MHz, CD₃CN) δ 161.74, 158.12, 157.93, 149.26, 148.58, 131.61(2C), 131.06, 130.98(2C), 124.64, 119.92(2C), 119.60(2C), 66.96(2C), 54.52, 48.06(2C), 35.57. Purity of 90% as determined by LC-MS.

***N*-methyl-1-(morpholine-4-carbonyl)-*N*-(3-phenoxybenzyl)-1*H*-1,2,4-triazole-3-sulfonamide (22)**

The title compound was synthesized from *N*-methyl-1-(morpholine-4-carbonyl)-1*H*-1,2,4-triazole-3-sulfonamide (**18a**, 240 mg, 0.87 mmol) and commercially available 3-phenoxybenzyl chloride (161 μL, 0.87 mmol) according to procedure described for compound **18**. This yielded *N*-methyl-1-(morpholine-4-carbonyl)-*N*-(3-phenoxybenzyl)-1*H*-1,2,4-triazole-3-sulfonamide (67 mg, 1.46 mmol, 17%). HRMS (ESI+) *m/z*: calculated for C₂₁H₂₄N₅O₅S ([M + H]), 458.1493; found, 458.1491. ¹H NMR (400 MHz, CD₃CN) δ 8.88 (s, 1H), 7.40-7.34 (m, 3H), 7.17-7.10 (m, 2H), 7.03-6.92 (m, 4H), 4.37 (s, 2H), 3.71 (brs, 8H), 2.30 (s, 3H). ¹³C NMR (101 MHz, CD₃CN) δ 161.60, 149.21, 148.50, 158.79, 157.86, 139.06, 131.14(2C), 130.92, 124.56, 124.04, 119.72(2C), 119.25, 118.95, 66.90(2C), 54.72, 47.39(brs, 2C), 35.71. Purity of 95% as determined by LC-MS.

2-(3-Formylphenoxy)-5-(trifluoromethyl)pyridine (26)

The title compound was synthesized from commercially available 3-hydroxybenzaldehyde (671 mg, 5.5 mmol), 2-chloro-5-trifluoromethylpyridine (1.0 g, 5.5 mmol) and K₂CO₃ (1.54 g, 8.5 mmol) according to previously published procedures²³ to obtain 2-(3-formylphenoxy)-5-(trifluoromethyl)pyridine (1.47 g, 5.5 mmol, 100%). ¹H NMR (400 MHz, CDCl₃) δ 10.03 (s, 1H), 8.42 (t, *J* = 0.8 Hz, 1H), 7.96 (dd, *J* = 8.8, 2.4 Hz, 1H), 7.78 (dt, *J* = 7.6, 1.2 Hz, 1H), 7.69-7.68 (m, 1H), 7.62 (t, *J* = 8.0 Hz, 1H), 7.45 (dq, *J* = 8.0, 1.2 Hz, 1H), 7.11 (d, *J* = 8.8 Hz, 1H). Spectroscopic data are in agreement with those reported in literature.²³

3-(5-Trifluoromethyl-2-pyridyloxy)benzyl alcohol (27)

The title compound was synthesized from 2-(3-formylphenoxy)-5-(trifluoromethyl)pyridine (**26**, 1.47 g, 5.5 mmol) according to procedures described for compound **24**. This yielded 3-(5-trifluoromethyl-2-pyridyloxy)benzyl alcohol (1.16 g, 4.3 mmol, 78%). ¹H NMR (400 MHz, CDCl₃) δ 8.40 (q, *J* = 0.8 Hz, 1H), 7.90 (dd, *J* = 8.8, 2.4 Hz, 1H), 7.40 (t, *J* = 8.0 Hz, 1H), 7.23 (dd, *J* = 12.0, 0.4 Hz, 1H), 7.16 (s, 1H), 7.05 (dd, *J* = 8.0, 2.0 Hz, 1H), 7.00 (d, *J* = 8.8 Hz, 1H), 4.68 (s, 2H). ¹³C NMR (101 MHz, CDCl₃) δ 165.87, 153.46, 145.51 (q, *J* = 4 Hz), 143.38, 136.90 (q, *J* = 3.0 Hz), 130.01, 132.92, 123.85 (q, *J* = 271.5 Hz), 122.50, 121.67 (q, *J* = 33.5 Hz), 119.84, 111.55, 64.66.

2-(3-(Bromomethyl)phenoxy)-5-(trifluoromethyl)pyridine (28)

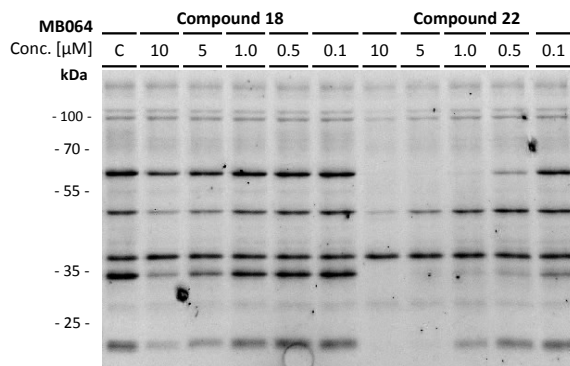
The title compound was synthesized from 3-(5-trifluoromethyl-2-pyridyloxy)benzyl alcohol (**27**, 1.16 g, 4.3 mmol) according to procedure described for compound **25**. This yielded 2-(3-(bromomethyl)phenoxy)-5-(trifluoromethyl)pyridine (1.25 g, 3.8 mmol, 88%). ¹H NMR (400 MHz, CD₃CN) δ 8.45 (d, *J* = 0.8 Hz, 1H), 7.91 (dd, *J* = 8.8, 2.4 Hz, 1H), 7.40 (t, *J* = 8.0 Hz, 1H), 7.29-7.27 (m, 1H), 7.21 (t, *J* = 2.0 Hz, 1H), 7.10 (dd, *J* = 2.4, 0.8 Hz, 1H), 7.02 (d, *J* = 8.8 Hz, 1H), 4.49 (s, 2H). ¹³C NMR (101 MHz, CD₃CN) δ 165.61, 153.34, 145.50 (q, *J* = 4.0 Hz), 139.81, 136.98 (q, *J* = 3.0 Hz), 130.25, 126.17, 123.71 (q, *J* = 271.5 Hz), 122.17, 121.83 (q, *J* = 33.7 Hz), 121.59, 111.59, 33.64.

N-methyl-1-(morpholine-4-carbonyl)-N-(3-((5-(trifluoromethyl)pyridin-2-yl)oxy)benzyl)-1H-1,2,4-triazole-3-sulfonamide (23)

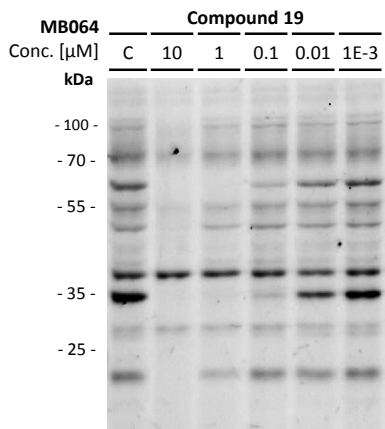
The title compound was synthesized from *N*-methyl-1-(morpholine-4-carbonyl)-1H-1,2,4-triazole-3-sulfonamide (**18a**, 240 mg, 0.87 mmol) and 2-(3-(bromomethyl)phenoxy)-5-(trifluoromethyl)pyridine (**28**, 319 mg, 0.96 mmol) according to procedure described for compound **18**. This yielded *N*-methyl-1-(morpholine-4-carbonyl)-*N*-(3-((5-(trifluoromethyl)pyridin-2-yl)oxy)benzyl)-1H-1,2,4-triazole-3-sulfonamide (86 mg, 0.16 mmol, 18%). HRMS (ESI+) *m/z*: calculated for C₂₁H₂₂F₃N₆O₅S ([M + H]), 527.1315; found, 527.1319. ¹H NMR (400 MHz, CDCl₃) δ 8.88 (s, 1H), 8.43 (s, 1H), 7.93 (dd, *J* = 8.7, 2.5 Hz, 1H), 7.43 (t, *J* = 7.9 Hz, 1H), 7.30 – 7.21 (m, 1H), 7.17 (t, *J* = 1.9 Hz, 1H), 7.12 (dd, *J* = 8.2, 2.4 Hz, 1H), 7.04 (d, *J* = 8.6 Hz, 1H), 4.48 (s, 2H), 4.08 – 3.68 (m, 8H), 2.91 (s, 3H). ¹³C NMR (101 MHz, CDCl₃) δ 165.62, 161.61, 153.58, 148.20, 147.39, 145.51 (q, *J* = 8.6 Hz), 137.39, 136.93, 130.21, 125.38, 123.74 (q, *J* = 272.7 Hz), 121.82 (q, *J* = 33.3 Hz), 121.40, 121.38, 111.66, 66.53(2C), 54.36, 46.99 (2C, bd, *J* = 215.5 Hz), 35.15. Purity of 98% as determined by LC-MS.

Supplementary information

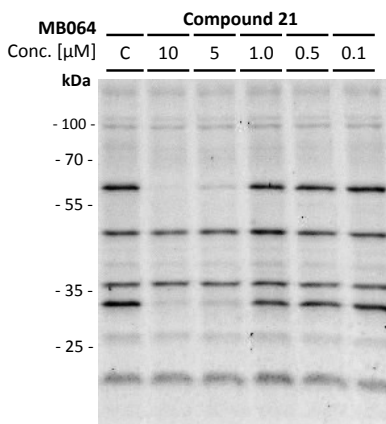
Representative gels of *in vitro* ABPP analysis on compounds **18-21** and *in vivo* ABPP analysis on spleen and testes on compounds **22** and **23**.



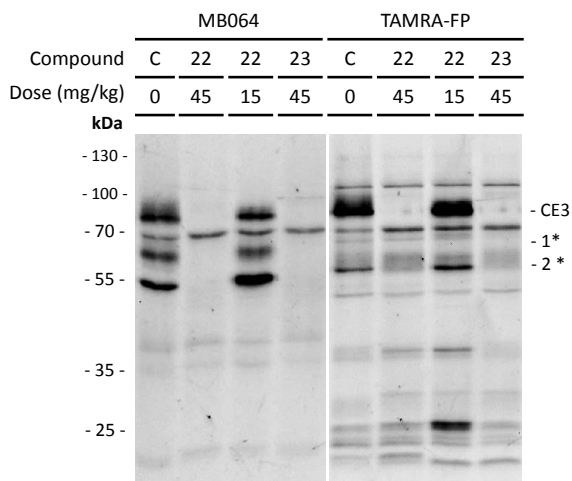
SI Figure 6. Representative gels of the ABPP analysis of compound **18** (left) and **20** (right) with ABP MB064. Conditions were used as described in the experimental section.



SI Figure 7. Representative gels of the ABPP analysis of compound **19** with ABP MB064. Conditions were used as described in the experimental section.



SI Figure 8. Representative gels of the ABPP analysis of compound **21** with ABP MB064. Conditions were used as described in the experimental section.



SI Figure 9: Representative gels of the *in vivo* characterization of compounds **22** and **23** with ABPs MB064 and TAMRA-FP on mouse spleen. Several off-targets were identified in the spleen using ABP MB064, including CE3 and two unknowns. Unknown 1*, however, is likely to be spleen ABHD16A as the apparent MW is in the expected kD range, although this should be further investigated by pull-down and mass spectrometry based proteomics using a biotin tagged ABP. Similar off-target effects were observed with TAMRA-FP (panel 2).

References

1. Vance, J. E. Phosphatidylserine and phosphatidylethanolamine in mammalian cells: two metabolically related aminophospholipids. *J. Lipid Res.* **49**, 1377–87 (2008).
2. Schlegel, R. a & Williamson, P. Phosphatidylserine, a death knell. *Cell Death Differ.* **8**, 551–563 (2001).
3. Newton, A. C. Protein Kinase C : Structure , Function, and Regulation. *J. Biol. Chem.* **270**, 1–52 (2003).
4. Lentz, B. R. Exposure of platelet membrane phosphatidylserine regulates blood coagulation. *Prog. Lipid Res.* **42**, 423–438 (2003).
5. Kamat, S. S. *et al.* Immunomodulatory lysophosphatidylserines are regulated by ABHD16A and ABHD12 interplay. *Nat. Chem. Biol.* **11**, 164–71 (2015).
6. Bellini, F. & Brunib, A. Role of a serum phospholipase A1 in the phosphatidylserine-induced T cell inhibition. *FEBS Lett.* **316**, 4–7 (1993).
7. Martin, T. W. & Lagunoff, D. Interactions of lysophospholipids and mast cells. *Nature* **279**, 250–252 (1979).
8. Smith, G. A., Hesketh, T. R., Plumb, R. W. & Metcalfe, J. C. The exogenous lipid requirement for histamine release from rat peritoneal mast cells stimulated by concanavalin A. *FEBS Lett.* **105**, (1979).
9. Lourens, S. & Blennerhassett, M. G. Lysophosphatidylserine potentiates nerve growth factor-induced differentiation of PC12 cells. *Neurosci. Lett.* **248**, 77–80 (1998).
10. Lord, C. C., Thomas, G. & Brown, J. M. Mammalian alpha beta hydrolase domain (ABHD) proteins: Lipid metabolizing enzymes at the interface of cell signaling and energy metabolism. *Biochim. Biophys. Acta - Mol. Cell Biol. Lipids* **1831**, 792–802 (2013).
11. Ramnani, N. The primate cortico-cerebellar system: anatomy and function. *Nat. Rev. Neurosci.* **7**, 511–22 (2006).
12. Hsieh, Y.-Y. *et al.* Human lymphocyte antigen B-associated transcript 2, 3, and 5 polymorphisms and haplotypes are associated with susceptibility of Kawasaki disease and coronary artery aneurysm. *J. Clin. Lab. Anal.* **24**, 262–8 (2010).
13. Savinainen, J. R. *et al.* Biochemical and pharmacological characterization of the human lymphocyte antigen B-associated transcript 5 (BAT5/ABHD16A). *PLoS One* **9**, 1–17 (2014).
14. van der Kleij, D. *et al.* A novel host-parasite lipid cross-talk. Schistosomal lyso-phosphatidylserine activates toll-like receptor 2 and affects immune polarization. *J. Biol. Chem.* **277**, 48122–48129 (2002).
15. Blankman, J. L., Long, J. Z., Trauger, S. a, Siuzdak, G. & Cravatt, B. F. ABHD12 controls brain lysophosphatidylserine pathways that are deregulated in a murine model of the neurodegenerative disease PHARC. *Proc. Natl. Acad. Sci. USA* **110**, 1500–1505 (2013).
16. Fiskerstrand, T. *et al.* A novel Refsum-like disorder that maps to chromosome 20. *Neurology* **72**, 20–27 (2009).
17. Fiskerstrand, T. *et al.* Mutations in ABHD12 cause the neurodegenerative disease PHARC: An inborn error of endocannabinoid metabolism. *Am. J. Hum. Genet.* **87**, 410–417 (2010).
18. Hoover, H. S., Blankman, J. L., Niessen, S. & Cravatt, B. F. Selectivity of inhibitors of endocannabinoid biosynthesis evaluated by activity-based protein profiling. *Bioorganic Med. Chem. Lett.* **18**, 5838–5841 (2008).
19. Baggelaar, M. P. *et al.* Development of an activity-based probe and in silico design reveal highly selective inhibitors for diacylglycerol lipase-a in brain. *Angew. Chem. Int. Ed.* **52**, 12081–12085 (2013).
20. Camara, K., Kamat, S. S., Lasota, C. C., Cravatt, B. F. & Howell, A. R. Combining cross-metathesis and activity-based protein profiling: New b-lactone motifs for targeting serine hydrolases. *Bioorganic Med. Chem. Lett.* **25**, 317–321 (2015).
21. Baggelaar, M. P. M. P. M. P. *et al.* A highly selective, reversible inhibitor identified by comparative chemoproteomics modulates diacylglycerol lipase activity in neurons. *J. Am. Chem. Soc.* **137**, (2015).
22. Johnson, D. S. *et al.* Discovery of PF-04457845: A highly potent, orally bioavailable, and selective urea FAAH inhibitor. *ACS Med. Chem. Lett.* **2**, 91–96 (2011).
23. Janssen, F. J. *et al.* Discovery of glycine sulfonamides as dual inhibitors of sn-1-diacylglycerol lipase α and α/β hydrolase domain 6. *J. Med. Chem.* **57**, 6610–6622 (2014).
24. Janssen, F. J. *et al.* Comprehensive Analysis of Structure-Activity Relationships of α -Ketoheterocycles as sn-1-Diacylglycerol Lipase α Inhibitors. *J. Med. Chem.* **58**, 9742–9753 (2015).